The compatible solute-binding protein OpuAC from *Bacillus subtilis*: ligand-binding, site directed mutagenesis and crystallographic studies

Sander H.J. Smits [1, ‡], Marina Höing [2, ‡], Justin Lecher [1], Mohamed Jebbar [3, +], Lutz Schmitt [1,*] and Erhard Bremer [2]

‡: Both authors contributed equally to this work

1) Institute of Biochemistry, Heinrich Heine University Duesseldorf, Universitätsstr. 1, 40225 Düsseldorf, Germany

2) Laboratory for Microbiology, Department of Biology, Philipps University Marburg, Karl-von-Frisch Str., 35032 Marburg, Germany

3) Departement Osmoregulation chez les Bacteries, Universite de Rennes 1, UMR-CNRS 6026, Rennes, Frances

+ Present address: Laboratory of Extreme Environments, Microbiology, University of West Brittany (Brest), European Institute of Marine studies, Technopôle Brest-Iroise, F-29280 Plouzané, France

Running title: Analyzing the ligand-binding site of OpuAC

Proposed section: Genetics and Molecular Biology

* Corresponding author:
Lutz Schmitt
Institute of Biochemistry
Heinrich Heine University Duesseldorf
Universitätsstr. 1
40225 Düsseldorf, Germany
Phone: +49(0)211-81-10773
Fax: +49(0)211-81-15310
Email: lutz.schmitt@uni-duesseldorf.de

Abstract

In the soil bacterium *Bacillus subtilis*, five transport systems work in concert to mediate the import of various compatible solutes that counteract the deleterious effects of increases in the osmolarity of the environment. Among these five systems, the ABC transporter OpuA, which catalyses the import of glycine betaine and proline betaine has been studied in detail in the past. Here, we demonstrate that OpuA is capable of importing the sulfobetaine dimethylsulfonioacetate (DMSA). Since OpuA is a classic ABC importer that relies on a substrate-binding protein priming the transporter with specificity and selectivity, we analyzed the OpuA-binding protein, OpuAC, by structural and mutational means with respect to DMSA binding. The determined crystal structures of OpuAC in complex with DMSA at 2.8 Å resolution and a detailed mutational analysis of these residues revealed a hierarchy within the amino acids participating in substrate binding. This finding is different to other binding proteins that recognize compatible solutes. Furthermore important principles that enable OpuAC to specifically bind various compatible solutes were uncovered.

INTRODUCTION

The soil bacterium *Bacillus subtilis* is equipped with five transport systems (Opu: osmoprotectant uptake) that allow the import of a large number of compatible solutes (4, 5, 25). Compatible solutes are low-molecular weight organic osmolytes that balances the osmotic potential of the cytoplasm with that of the environment. Three of the five compatible solutes transport systems (OpuA, OpuC and OpuD) mediate the uptake of the widespread found osmoprotectant glycine betaine (22, 24). Glycine betaine can also be synthesized by *B. subtilis* from the precursor choline (3), which is acquired from the environment via the osmoregulated OpuB and OpuC transporters (23). The Opu transport systems also mediate the osmoregulated uptake of several other compatible solutes (4, 19, 25). For instance, proline betaine is taken up by *B. subtilis* via the OpuA and OpuC transporters (B. Kempf and E. Bremer; unpublished results).

OpuD is a secondary transporter that belongs to the BCCT-family (Betaine-Choline-Carnitine-Transporter) of uptake systems (22). In contrast, OpuA, OpuB and OpuC are members of the ABC-(ATP binding cassettes) transporters, which use the energy released by ATP hydrolysis to transport substrates against a concentration gradient (16, 42). In general, ABC-transporters are composed of four modules. The two nucleotide-binding domains and two transmembrane domains can be arranged in any possible combination. However, ABC-import

77 systems such as OpuA, OpuB and OpuC contain a fifth module, a substrate-
78 binding protein. This substrate-binding protein captures the substrate with high
79 affinity and delivers it to the cognate transport system for subsequent ATP-
80 dependent import. In Gram-negative bacteria binding proteins diffuse freely in the
81 periplasmic space, while they are lipid-anchored in the cytoplasmic membrane in
82 Gram-positive bacteria such as *B. subtilis*, (1, 24, 26). However, it was recently
83 shown that binding proteins can even be fused to the transmembrane domain of
84 the ABC-transporter (36, 43).
85
86 Despite this variation, all substrate-binding proteins from ABC-transporters
87 analyzed by X-ray crystallography today display a bilobal architecture. The
88 ligand-binding site is located in a deep cleft situated between these two lobes
89 and residues located on both lobes usually contribute to substrate binding (45).
90 Based on structural and kinetic investigations, a “Venus fly-trap” mechanism was
91 proposed to explain the ligand-binding mechanism on a molecular level (32, 39).
92 Here, substrate-binding proteins undergo constant opening-closing motions in the
93 absence of the ligand and the amino acids connecting both domains act as pivot
94 point in such a hinge-bending motion. Upon ligand binding, the equilibrium
95 between the open and closed state of the binding protein is shifted towards the
96 so-called “liganded-closed” state and the ligand is bound in a cleft located
97 between both domains.
98
99 The ABC transporter OpuA from *B. subtilis* (19) has been analyzed

functionally and structurally by *in vivo* or *in vitro* studies of either the whole transporter or its isolated components (17, 18, 20, 24, 26). The OpuA system consists of the cytoplasmic membrane-associated ATPase OpuAA (18), the integral membrane transport component OpuAB (17) and the extracellular ligand binding protein OpuAC (24). This latter protein is tethered to the cytoplasmic membrane via a lipid modification at its amino-terminus (26). The crystal structure of OpuAC in complex with two ligands, glycine betaine or proline betaine, has been reported recently (20). The ligand-binding pocket of OpuAC is formed by three tryptophan residues arranged in a “prism-like” geometry suitable to coordinate the positive charge of the trimethylammonium group of glycine betaine or the dimethylammonium group of proline betaine by cation-π interactions. Additionally, hydrogen bonds with the carboxylate moiety of the ligand are formed. Structural differences between the OpuAC/glycine betaine and OpuAC/proline betaine complexes occur within the ligand-binding pocket that allow a structural explanation for the drastic affinity differences of OpuAC for these two ligands. The K_D for the binding of glycine betaine by OpuAC is 17 ± 1 µM, whereas the K_D for the binding of proline betaine is 295 ± 27 µM (20).

Dimethylsulfonioacetate (DMSA), the closest sulfonium analog of glycine betaine (Fig. 1) is found as a secondary osmolyte in certain species of marine algae (7, 9). Previous studies have shown that DMSA (also referred to as sulfobetaine or dimethylthetin) (7) can function as an osmoprotectant for *E. coli* where it is accumulated via the ProP and ProU compatible solute uptake systems

(9). DMSA also serves as an osmoprotectant for *Pseudomonas aeruginosa* PAO1 (10) and the lactic acid bacterium *Tetragenococcus halophila* (2). Furthermore, DMSA is a substrate for the periplasmic binding protein from the glycine betaine and choline transporter OusB from *Erwinia crysanthemi* (8). Interestingly, uptake of DMSA in *Sinorhizobium meliloti* is toxic and it becomes only osmoprotective in mutants that are unable to dimethylate this sulfobetaine (38).

To further analyze the binding principles of compatible solutes to OpuAC, it is desirable to assess the importance of single tryptophans participating in the formation of the Trp-prism and other amino acids contributing to ligand binding (20). Therefore, we have performed a mutational study of the ligand binding-site. Furthermore, we present the crystal structure of OpuAC in complex with the compatible solute dimethylsulfonioacetate (DMSA), an efficient osmoprotectant for *B. subtilis* and a substrate of the OpuA transporter.

MATERIALS AND METHODS

Bacterial strains, plasmids and culture conditions. The *E.* coli strains used in this study were maintained on Luria-Bertani medium (33) and were propagated at 37°C. For the selection of *E. coli* strains carrying derivatives of the expression vector pASK-IBA6 (IBA, Göttingen, Germany), ampicillin (100 µg ml^{-1}) was added to the liquid cultures and agar plates. Overproduction of the *B. subtilis* OpuAC protein and its mutant derivatives was carried out in the *E. coli* strain BL21 (*F⁻ gal met r⁻ m⁻ hsdS*(λDE3) (Stratagene, La Jolla, CA, USA). For OpuAC overproduction, the plasmid-carrying BL21 strain was propagated in a defined minimal medium (MMA) (33) supplemented with 100 µg ampicillin ml^{-1}, 0.2% (w/v) Casamino Acids and 0.5 % (w/v) of glucose as carbon source. Mutant derivatives of the *opuAC*-expression plasmid pMH24 were recovered after transformation into Epicurian coli® XL1-Blue (*recA1 endA1 gyrA96 thi-1 hsdR17 supE44 relA1 lac* [F´ *proAB lac1^{q}*ZΔ*M15*Tn*10*(Tet^{r})]) (Stratagene, La Jolla, CA, USA). The *B. subtilis* strains RMKB24 [Δ(*opuA::erm*)4 Δ(*opuBD::tet*)23 *opuC*-20::Tn*10*(*spc*) Δ(*opuD::neo*)2] and RMKB34 [*opuA*$^{+}$ Δ(*opuBD::tet*)23 *opuC*-20::Tn*10*(*spc*) Δ(*opuD::neo*)2] are derivatives of the wild type strain JH642 (*trpC pheA1*) (J. Hoch, Scripps Research Institute, CA, USA). The genetic construction of these two *B. subtilis* mutants has been described by Kappes *et al.* (23).

B. subtilis strains were grown in Spizizen´s minimal medium (SMM) with 0.5% (w/v) glucose as the carbon source and supplemented with L-tryptophan

161 (20 µg ml^{-1}), L-phenylalanine (18 µg ml^{-1}) and a solution of trace elements (15).
162 When required, the osmotic strength of SMM was increased by the addition of
163 NaCl from a 5 M stock solution. Experiments that continuously monitored the
164 growth of the *B. subtilis* cultures, 20 ml pre-warmed SMM-Medium containing 1.2
165 M NaCl in a 100 ml Erlenmeyer flask was inoculated with a late-exponential-
166 phase pre-culture grown in SMM with 0.4 M NaCl to an OD_{578} of 0.1. These
167 cultures were grown in a shaking water bath (set at 200 rpm) at 37°C.
168 Compatible solutes (glycine betaine, proline betaine and dimethylsulfonioacetate)
169 were added to *B. subtilis* cultures to a final concentration of 1 mM each, as
170 required.
171
172 **Chemicals.** Glycine betaine was purchased from Sigma-Aldrich (Munich,
173 Germany), proline betaine was obtained from Extrasynthèse (Genay Cedex,
174 France) and dimethylsulfonioacetate was synthesized as described by Ferger
175 and Vigneaud (13).
176
177 **Overexpression and purification of the recombinant OpuAC protein in**
178 ***E. coli*.** Plasmid pMH24 is a *B. subtilis opuAC*$^+$ derivative of the expression
179 vector pASK-IBA6 (IBA, Göttingen, Germany). In this recombinant plasmid, the
180 *opuAC* coding region (without its own signal sequence and the codon specifying
181 the amino-terminal cysteine residue of the mature OpuAC protein) (26) is
182 positioned under the control of the anhydrotetracycline-inducible *tet* promotor
183 present in the vector pASK-IBA6. This allows induction of the transcription of the

184 *opuAC* gene to high levels in the host strain BL21. The *opuAC* coding region has
185 been inserted in pASK-IBA6 in-frame with an upstream *ompA* signal sequence
186 and the codons for a Strep-TagII affinity peptide. This allowed the secretion of the
187 Strep-TagII-OpuAC fusion protein into the periplasm of *E. coli* where it could be
188 released from by cold osmotic shock and recovered by affinity chromatography
189 on Strep-Tactin sepharose (IBA, Göttingen, Germany). Strain BL21(pMH24) in 5
190 liters defined MMA to an OD_{578} = 0.1 was inoculated from an overnight culture of
191 BL21(pMH24) prepared in the same medium. *opuAC* transcription was induced
192 at an OD_{578} = 0.7 of the culture by the addition of 0.2 µg ml^{-1} anhydrotetracycline.
193 Growth of the culture of BL21(pMH24) was then continued for 1.5 h at 37°C with
194 avid stirring. Subsequently, cells were harvested by centrifugation (10 min, 3,000
195 x g). To release periplasmic proteins from the BL21(pMH24) cells, the cell pellet
196 was re-suspended in 50 ml of ice-cold buffer P (50 mM Tris
197 (tris(hydroxymethyl)aminomethan)-HCl pH 8.0, 100 mM NaCl, 500 mM sucrose)
198 and incubated for 30 min on ice. Soluble periplasmic proteins were isolated by
199 two subsequent centrifugation steps. First, the supernatant was centrifuged for
200 15 min at 21,000 x *g* to remove cellular debris. Subsequently, the supernatant
201 was re-centrifuged for 60 min at 120,000 x *g* to remove denatured proteins. The
202 cleared, soluble periplasmic protein fraction was then loaded onto a 10 ml-Strep-
203 Tactin column (IBA, Göttingen, Germany), pre-equilibrated with 10 bed volumes
204 of buffer W (50 mM Tris-HCl, 100 mM NaCl, pH 8.0). After the column was
205 washed with 10 bed volumes of buffer W, bound proteins were eluted from the
206 affinity resin with buffer E (50 mM Tris-HCl pH 8.0, 100 mM NaCl, 2.5 mM

207 desthiobiotin). OpuAC containing fractions were collected in 5 ml portions.

208

209 Two forms of the recombinantly produced OpuAC were released from the
210 periplasmic fraction: (i) the non-processed OmpA-Strep-TagII-OpuAC fusion and
211 (ii) the processed Strep-TagII-OpuAC form. To remove the OmpA signal
212 sequence and the Strep-TagII from unprocessed OmpA-Strep-TagII-OpuAC and
213 the Strep-TagII from processed Strep-TagII-OpuAC, OpuAC containing fractions
214 were pooled and incubated overnight at 23°C with 0.5 U Factor Xa (Novagen,
215 Darmstadt, Germany) per 10 µg of OpuAC in buffer E in the presence of 4 mM
216 $CaCl_2$. Complete removal of the OmpA signal sequence and the Strep-TagII from
217 OpuAC was verified by SDS-PAGE. OpuAC was concentrated to a volume of
218 approximately 500 µl using VIVASPIN 4 (Vivascience, Hannover, Germany)
219 concentrator columns (exclusion size, 10 kDa). Subsequently, the protein was
220 passed through a HiTrapQ anion exchange column (GE Healthcare, Munich,
221 Germany) to remove Factor Xa from the protein preparation. The column was
222 washed with a buffer containing 25 mM Tris-HCl and 25 mM NaCl (pH 8.3).
223 OpuAC does not bind to the HiTrapQ material and passes through the column,
224 whereas Factor Xa bound to the HiTrapQ material. Finally, isolated OpuAC was
225 dialyzed against 2 x 5 liters of 10 mM Tris-HCl (pH 7.0) at 4°C overnight and
226 stored at 4°C until further use. In general, approximately 1.5 mg of pure OpuAC
227 protein was obtained per liter of *E. coli* culture. The functionality of the purified
228 OpuAC protein was assessed by fluorescence spectroscopy using changes in
229 the intrinsic tryptophan fluorescence of OpuAC upon substrate binding (e.g.

glycine betaine) as detailed by Horn *et al.* (20). Protein concentrations were estimated based on the theoretical molar extinction coefficient of OpuAC yielding the following correlation: A_{280}= 1.0 corresponds to 0.5 mg ml^{-1} OpuAC. OpuAC used for crystallization experiments was concentrated to approximately 10 mg ml^{-1} using VIVASPIN 4 (Vivascience, Hannover, Germany) concentrator columns (exclusion size, 10 kDa).

Site directed mutagenesis of the *opuAC* gene. To determine the individual contribution of the amino acids forming the Trp prism (Trp^{72}, Trp^{178} and Trp^{225}) and His^{230} to the stability of the OpuAC/glycine betaine, OpuAC/proline betaine and OpuAC/DMSA complexes (20), the corresponding codons in the *opuAC* gene were changed via site-directed mutagenesis using the QuikChange site directed-mutagenesis kit (Stratagene, La Jolla, CA, USA) and custom synthesized mutagenic primers (Biomers, Ulm, Germany). These experiments were conducted with the *opuAC*$^+$ plasmid pMH24. The entire coding region of the mutant *opuAC* genes was sequenced to ensure the presence of the desired mutation and the absence of undesired alterations in the *opuAC* coding region. Double and triple mutants were generated from the plasmids bearing the corresponding single or double mutations at the desired positions. The following mutant *opuAC* variants were generated on plasmid pMH24: pMH26 (Trp72→Ala [TGG→GCG]), pMH27 (Trp72→Phe [TGG→TTT]), pMH28 (Trp72→Tyr [TGG→TAT]), pMH29 (Trp178→Ala [TGG→GCG]), pMH30 (Trp178→Phe [TGG→TTT]), pMH31 (Trp178→Tyr [TGG→TAT]), pMH32 (Trp225→Ala [

253 TGG→GCG]), pMH33 (Trp225→Phe [TGG→TTT]), pMH34 (Trp225→Tyr
254 [TGG→TAT]), pMH35 (His230→Ala [CAT→GCG]), pMH36 (Trp72→Phe;
255 Trp178→Phe [TGG→TTT]), pMH37 (Trp72→Tyr; Trp178→Tyr [TGG→TAT]),
256 pMH38 (Trp72→Phe; Trp178→Phe, Trp225→Phe [TGG→TTT]), pMH39
257 (Trp72→Tyr; Trp178→Tyr; Trp225→Tyr [TGG→TAT]), pML1 (Trp72→Phe;
258 Trp225→Phe [TGG→TTT]), pML2 (Trp72→Tyr; Trp225→Tyr [TGG→TAT]). The
259 mutant *opuAC* genes were overexpressed in strain BL21 as described above for
260 the wild type *opuAC* gene. Mutant OpuAC proteins were then purified exactly as
261 described for wild type OpuAC. The mutant proteins were recovered with similar
262 yields as the wild type indicating that the introduced mutations in *opuAC* did not
263 alter the stability of the mutant proteins.
264
265 **Determination of the dissociation constants of the OpuAC/compatible**
266 **solute complexes.** The dissociation affinity of the OpuAC/glycine betaine,
267 proline betaine or DMSA complexes was determined as described by Horn *et al*.
268 (20). In brief, the intrinsic tryptophan fluorescence of OpuAC was monitored from
269 300 nm to 450 nm using a Cary Eclipse fluorescence spectrometer (Varian,
270 Surrey, UK). The excitation wavelength was set to 295 nm, slit width of 5 nm and
271 the temperature was maintained at room temperature (22 ± 1° C) using a
272 circulating water bath. Different amounts of the substrates were titrated to 1 ml
273 OpuAC samples (250 nM in 10 mM Tris-HCl, pH7.0) and fluorescence was
274 measured after equilibration (5 min). Changes in the maximum emission
275 wavelength (glycine betaine or proline betaine), determined by an automated

peak search routine, or changes in the fluorescence intensity (DMSA) were plotted against substrate concentration after background correction. Upon binding of glycine betaine or proline betaine to OpuAC, a blue shift of $\lambda_{em,max}$ from 345 nm in the absence of ligand to 336 nm under substrate saturation conditions was observed. The changes of the emission maxima or fluorescence intensity due to the concentration of bound substrates could by analyzed using a 1:1 binding site model employing equation 1 (glycine betaine and proline betaine) or equation 2 (DMSA):

$$\lambda_{em,max} = \lambda_{em,max0} + (\Delta\lambda_{em,max} * [S_0]/([S_0] + K_D)) \quad \text{equation 1}$$

Here, $\lambda_{em,max}$ is the emission wavelength maximum for a given substrate concentration; $\lambda_{em,max0}$ is the emission wavelength maximum without substrate; $\Delta\lambda_{em,max}$ is the maximal emission wavelength maximum shift; S_0 is the substrate concentration; K_D is the dissociation constant.

$$F = F_0 + (\Delta F * [S_0]/([S_0] + K_D)) \quad \text{equation 2}$$

Here, F is the fluorescence intensity for a given substrate concentration; F_0 is the fluorescence intensity without substrate; ΔF is the maximal change in fluorescence intensity; S_0 is the substrate concentration; K_D is the dissociation constant. All K_D measurements of OpuAC and its mutant derivatives that are summarized in Table 1 represent the average of at least three independent measurements, with a standard deviation given as errors.

Crystallization of the OpuAC/DMSA complex, data collection and

299 **model refinement.** Crystals of the OpuAC/DMSA complex were obtained under
300 conditions similar to the ones described for the glycine betaine and proline
301 betaine complexes (20). Prior to crystallization, OpuAC (at a concentration of 10
302 mg ml^{-1}) was incubated with 3 mM DMSA. Subsequently, 1 µl of protein solution
303 was mixed with 1 µl of reservoir solution and 0.5 µl of 100 mM L-cysteine. The
304 reservoir solution contained 100 mM Tris–HCl (pH 8.25), 150 mM NH_4OAc and
305 15% (w/v) PEG 4000. Crystal plates appeared at room temperature after several
306 weeks, with final dimensions of 200 µm x 100 µm x 30 µm. Crystals were
307 transferred into cryo-buffer (150 mM TrisHCl (pH 8.3), 20% (w/v) ethylene glycol,
308 200 mM NH_4OAc, 20% (w/v) PEG 4000) and flash-frozen in liquid nitrogen.
309 Diffraction data were collected at 100 K at the EMBL beam line BW7A at DESY,
310 Hamburg. Data were indexed and scaled with XDS and further analyzed using
311 the CCP4 program package (6). The structure was solved by molecular
312 replacement using AMORE (35) with the OpuAC/glycine betaine monomer (20)
313 as search model. Four monomers were found in the asymmetric unit and the
314 initial structure was further improved by manual rebuilding in $2F_o$-F_c and $1F_o$-F_c
315 electron density maps using COOT (12) and subsequent rounds of refinement
316 employing REFMAC5 (34). During the initial refinement cycles strict NCS
317 restrains (27) were maintained, which were released in the last five cycles of
318 refinement. The quality of the model was verified with the MolProbity server
319 (www. molprobity.biochem.duke.edu/) and is summarized in Table 2. R_F and R_{free}
320 values are 28.5 % and 36.4 %, respectively. Although at the higher end of the
321 range expected at this resolution (28), they are still within the limits and the

322 quality of the electron density map allowed a detailed analysis of the structure.

323

324 **Protein Data Bank Accession Code.** Coordinates of the OpuAC/DMSA
325 complex have been deposited in the RCSB Protein Data Bank under accession
326 code 3CHG .

RESULTS AND DISCUSSION

DMSA is a substrate for the OpuA transporter and confers osmoprotection in *B. subtilis*. Previous growth studies and transport assays have shown that DMSA is also an effective osmoprotectant for *B. subtilis* and is acquired by the cell via the OpuA, OpuC and OpuD osmolyte transport systems (G. Nau-Wagner, M. Jebbar and E. Bremer; unpublished results). Hence, glycine betaine (22-24) and its sulfur analog DMSA are taken up via the same three transport systems. We analyzed the uptake of DMSA via the OpuA transporter by growth experiments. Both glycine betaine and DMSA (provided at a concentration of 1 mM each) were very effective osmoprotectants in strain RMKB34 that is $OpuA^+$, but defective in the compatible solute uptake systems OpuB, OpuC and OpuD (Fig. 2A). When the OpuA system is inactivated by a gene disruption mutation in an otherwise $OpuB^-$, $OpuC^-$ and $OpuD^-$ background (RMKB24), osmoprotection by glycine betaine is completely blocked as has been reported previously by Kappes *et al.* (22) and osmoprotection by DMSA is greatly reduced (Fig. 2B). We conclude from these growth experiments, that DMSA is a substrate for the OpuA transporter, but that a fourth uptake route for DMSA seems to operate in *B. subtilis* that remains to be identified. Since DMSA can enter the cell via the OpuA system, this sulfobetaine should be recognized by the ligand-binding protein (OpuAC) of the OpuA transporter.

DMSA is bound by the purified *B. subtilis* OpuAC protein. We overexpressed the *B. subtilis opuAC* gene in *E. coli* and purified the recombinant OpuAC protein by affinity chromatography to homogeneity (data not shown). To determine the affinities of glycine betaine, proline betaine and DMSA to the purified OpuAC protein, an intrinsic Trp-fluorescence based binding assay was employed. A spectra and the corresponding binding curve for DMSA is shown in Figure 3. Binding of glycine betaine and proline betaine to OpuAC resulted in a blue shift of the emission spectra of 9 nm (glycine betaine, data not shown) and 6 nm (proline betaine, data not shown), respectively. This shift in emission maximum was subsequently used to determine the dissociation constants of the complexes according to equation 1 (see MATERIALS AND METHODS). A 1:1 binding isotherm described the experimental data adequately and K_D values could be calculated to 22 ± 4 µM and to 267 ± 6 µM for glycine betaine and proline betaine, respectively (Table 1). These values are in very good agreement with those previously determined (glycine betaine: K_D= 17 ± 1 µM; proline betaine: K_D= 295 ± 27 µM) for these two OpuAC substrates by Horn *et al*. (20). In contrast to the binding of glycine betaine and proline betaine to OpuAC, binding of DMSA to OpuAC did only induce a marginal blue shift of the emission maximum (2 nm; data not shown). Therefore, the decrease in fluorescence intensity was used to determine the binding constant according to equation 2 (see MATERIALS AND METHODS) assuming again a 1:1 binding isotherm (Fig. 3B). Here, a calculated K_D value of 102 ± 11 µM was determined, an affinity that is between the values determined for the other two OpuAC ligands (Table 1).

From a chemical point of view, the structures of the individual ligands (Fig. 1) do not provide any ready explanation for these differences in affinity. All three ligands contain a carboxylate moiety and a delocalized positive charge. Since the K_D value of DMSA is in between the one for glycine betaine and proline betaine, the nature of the delocalized positive charge does not seem to be relevant for the apparent affinity differences (Table 1).

Crystal structure of OpuAC with its ligand DMSA. To gain inside into the molecular determinants that govern binding of DMSA by OpuAC, we crystallized this ligand-binding protein in the presence of DMSA and determined the crystal structure of the OpuAC/DMSA complex at a resolution of 2.8 Å. The structure was solved by molecular replacement using the recently determined OpuAC/glycine betaine structure (20) as a search model and refined using REFMAC5 (34). A summary of the data collection statistics and refinement details as well as the model content are given in Table 2. As expected, the overall fold of OpuAC in complex with DMSA (RCSB Protein Data Bank accession code 3CHG) is similar to that of the recently published OpuAC complexes containing either glycine betaine (RCSB Protein Data Bank accession code 2B4L) or proline betaine (RCSB Protein Data Bank accession code 2B4M), respectively (20). The OpuAC/DMSA complex exhibits the characteristic bilobal protein fold observed for many binding proteins of prokaryotic ABC transport systems (32, 39, 45).

394 The quality of the initial electron density map of the OpuAC protein with the
395 bound DMSA allowed an unambiguous placement of the ligand and thereby the
396 localization of the sulfonium moiety of DMSA despite the medium resolution (2.8
397 Å) of the overall OpuAC/DMSA structure. In contrast to the structure of the
398 OpuAC/glycine betaine complex (20), the asymmetric unit of the OpuAC/DMSA
399 crystal structure contained four protomers. Since the root mean square deviation
400 of the individual protomers in the asymmetric unit was smaller than 1 Å, the
401 description of the structure will be restricted to a single protomer (monomer D).
402 Two of these protomers are related via non-crystallographic symmetry, which
403 was used during the initial steps of structure refinement but released in the last
404 cycles of refinement. As shown in Fig. 4, the overall architecture of the DMSA
405 binding site was identical to the OpuAC/glycine betaine complex (20) and is
406 composed of three tryptophans (Trp^{72}, Trp^{178}, Trp^{225}) and one histidine (His^{230}).
407 Additionally, the carboxylate of DMSA interacts with the backbone amids of Gly^{26}
408 and Ile^{27} via hydrogen bonds (3.5 Å and 2.9 Å, respectively), as has been
409 previously observed both in the OpuAC/glycine betaine and OpuAC/proline
410 betaine complexes (20). These two hydrogen bonds together with the interaction
411 of DMSA with His^{230} (distance of 3.2 Å) fix the carboxylate moiety of DMSA within
412 the ligand-binding site (Fig. 4). The dimethylsulfonium group of DMSA interacts
413 with the individual tryptophans of the “Trp-prism” (Trp^{72} Trp^{178} Trp^{225}) (20) via
414 cation-π interactions (31). All distances range between 3.5-4.0 Å, perfectly fitting
415 the van der Waals interactions and fulfilling the requirements of cation-π
416 interactions (30). However, a closer inspection reveals that only 19 cation-π

417 interactions and 6 van der Waals interactions are present in the DMSA complex,
418 while 22 cation-π interactions were determined for the OpuAC/glycine betaine
419 complex (20). In contrast, only 6 cation-π and 15 van der Waals interactions are
420 found in the OpuAC/proline betaine complex (13). More important, however, is
421 the fact that the interaction distance between His^{230} and the ligands glycine
422 betaine, DMSA and proline betaine is 2.6 Å, 3.5 Å and 4.7 Å, respectively. The
423 distance of His^{230} to proline betaine is even beyond the effective distance of a
424 salt bridge. Horn *et al.* (20) used this distance argument, to explain the drastically
425 lower affinity of OpuAC for proline betaine (K_D = 295 µM ± 27 µM) compared to
426 the affinity of OpuAC for glycine betaine (K_D = 17 µM ± 1 µM). In light of the
427 OpuAC/DMSA structure reported here and the previously reported analysis of the
428 OpuAC/glycine betaine and OpuAC/proline betaine complexes (20), the
429 combination of different numbers of cation-π and van der Waals interactions
430 contribute significantly to ligand binding. Furthermore, important for substrate
431 binding appears also the presence (in the case of glycine betaine and DMSA) or
432 the absence (in the case of proline betaine) of an interaction between the ligand
433 and His^{230}.

434 To compare the positioning of the three OpuAC substrates within the ligand
435 binding sites, we superimposed the OpuAC/glycine betaine, OpuAC/proline
436 betaine and OpuAC/DMSA crystal structures. As shown in Figure 5, the ligand-
437 binding site of OpuAC/DMSA complex matches almost perfectly the
438 OpuAC/glycine betaine and the OpuAC/proline betaine structure. Next to the
439 slightly different conformations of His^{230} in the three structures (Fig. 5), the

most important difference between the OpuAC structures is the conformation of the indole moiety of Trp^{178}. In the OpuAC/proline betaine complex, it is flipped nearly 180° with respect to the position in the OpuAC/DMSA and the OpuAC/glycine betaine complex. Thus, it is tempting to speculate that the orientation of this side chain might contribute to the overall affinity of OpuAC to either its high-(glycine betaine), medium-(DMSA) or low-affinity (proline betaine) ligands.

Site-directed mutagenesis of the OpuAC ligand-binding pocket. The analysis of the three OpuAC structures in complex with the various ligands provides a molecular framework to describe the interactions and affinities of different compatible solutes to OpuAC. To analyze the contribution of individual amino acid residues within the OpuAC binding pocket to ligand binding, we performed a site-directed mutagenesis study. We mutagenized the *opuAC*$^+$ overexpression plasmid pMH24 using the QuikChange site directed-mutagenesis kit (Stratagene) and a set of mutagenic DNA-primers. In total, we generated 16 *opuAC* mutants (see MATERIALS AND METHODS). Each of these mutant *opuAC* genes were overexpressed in strain BL21 and the variant OpuAC proteins were purified to homogeneity by affinity chromatography. The purified mutant OpuAC proteins were analyzed for binding and affinity to glycine betaine, proline betaine and DMSA by using fluorescence spectroscopy and these data are summarized in Table 1. For a structural summary see Figure 4.

462 The generated mutations can be principally sub-divided into four classes: (i)
463 The three tryptophan residues forming the "Trp-prism" (Trp^{72}, Trp^{178}, and Trp^{225})
464 were mutated individually to alanine residues. (ii) The three Trp residues were
465 separately mutated to either phenylalanine or tyrosine residues. (iii) We also
466 simultaneously changed the three tryptophan residues forming the "Trp-prism" to
467 either Phe or Tyr. (iv) His^{230} was substituted to alanine.

468 To determine the influence of Trp-residues within the OpuAC binding site on
469 complex stability, we assessed individual Ala substitutions for substrate binding.
470 As shown in Table 1, mutation of any of the three tryptophans to alanine resulted
471 in a complete loss of ligand binding. This is different from the situation found in
472 the glycine betaine/proline betaine binding protein ProX from *E. coli*. Here, three
473 Trp-residues, arranged in a "box-like" structure, constitute the binding surface for
474 the trimethlyammonium headgroup of glycine betaine and the
475 dimethylammonium-headgroup of proline betaine via cation-π interactions (40).
476 Two of these Trp-residues (Trp^{65} and Trp^{140}) can be changed to Ala-residues
477 with modest effects on substrate binding. However, the replacement of Trp^{188}
478 with Ala results in a complete loss of binding of glycine betaine (40).
479 Consequently, in the "box-like" arrangement of the Trp-residues found within the
480 binding site of ProX, only a single Trp-residue is critical for substrate binding. The
481 other two Trp-residues appear to stabilize the substrate within the ligand-binding
482 pocket (33).

483 As elaborated by Dougherty and co-workers (11, 31), the strength of a

484 cation-π interaction between a ligand and a protein decreases from Trp to Tyr to
485 Phe, thus following the decrease in the electronegative potential of the indole,
486 phenole and benzole side chain of the amino acids. We therefore individually
487 changed Trp^{72}, Trp^{178} and Trp^{225} of OpuAC to either Phe or Tyr-residues.
488 Exchange of a single tryptophan to either Phe or Tyr resulted in a complex
489 response with respect to ligand binding and this was dependent on the
490 tryptophan mutated and the ligand analyzed (Table 1). These substitutions
491 caused in general substantial decreases in affinity of OpuAC for its three ligands
492 and in several cases no substrate binding could be detected at all (Table 1). This
493 result is surprising, since the site-directed change of the Trp-residues to either
494 Phe- or Tyr-residues within the *E. coli* ProX ligand binding site, has essentially no
495 influence on ligand binding (40). Furthermore, mutational analysis of the aromatic
496 residues within the binding site of the ectoine/hydroxyectoine binding protein
497 EhuB from *Sinorhizobium meliloti* (14, 21) revealed that the strength of the
498 cation-π interaction is of key importance for the efficiency of substrate binding.
499 An aromatic box composed of Phe^{24}, Tyr^{60} and Phe^{80} forms a central part of the
500 ligand binding site of the EhuB protein allowing substrate binding with K_D values
501 in a low µM range (14). Substitutions of these aromatic residues by Trp, the
502 amino acid with the strongest electronegative potential and hence best suited for
503 cation-π interactions (11, 31), created super-binding variants of EhuB that bind
504 both ectoine and hydroxyectoine with K_D values in a low nM range (14).

505 Simultaneous change of either two tryptophans ($Trp^{72/178}$, $Trp^{72/225}$ or
506 $Trp^{178/225}$) or all three tryptophans to either Phe- or Tyr-residues completely

abolished ligand binding (Table 1). This clearly demonstrates that a single Trp-residue paired with two other aromatic amino acids is not sufficient for OpuAC to bind any of the three substrates tested. We are thus tempted to speculate that the "Trp-prism" found in OpuAC has been evolutionary optimized for ligand binding in such a way that only minor variations are permitted. This argument is strengthened by our data base searches. We aligned the amino acid sequence of 64 OpuAC related proteins (Figure 6) and found that Trp^{72}, Trp^{178} and Trp^{225} are completely conserved, regardless whether the proteins align directly with OpuAC, whether the alignment requires the inversion of N- and C-terminal domains (20) or whether the ligand-binding portion is fused to the transmembrane domain of the corresponding ABC transport systems (Figure 6; further details are provided in the Figure legend).

A rather surprising result is obtained when Trp^{178} is changed to Tyr. This substitution causes a drastic decrease in glycine betaine binding, abolishes DMSA binding, but increases substantially the binding of proline betaine. Currently, we have no biochemical or structural explanation for these findings.

The analysis of the crystal structures of the OpuAC/glycine betaine and OpuAC/proline betaine complexes suggested that an additional hydrogen bond between the carboxylate of glycine betaine and His^{230} was responsible for the 17fold higher affinity of OpuAC for glycine betaine than for proline betaine (20). In a His^{230} to Ala substitution, this critical hydrogen bond will be abolished, thus predicting that the binding affinity of OpuAC for glycine betaine should be

529 strongly decreased and should approach that of proline betaine. The data
530 summarized in Table 1 demonstrate that this is indeed the case and thus support
531 the prediction made by Horn *et al.* (20) based on the interpretation of the OpuAC
532 structures. Since His^{230} makes also contacts to the carboxylate of DMSA binding
533 of the sulfobetaine is also substantially reduced by the replacement of His^{230} with
534 Ala (Table 1). These findings are consistent with the view that interactions
535 between the carboxylate of the ligands and His^{230} make important contributions
536 to the overall affinity of the OpuAC protein to its ligands. Thus, His^{230} has a prime
537 role in modulating affinity of the OpuAC/compatible solute complexes. Although
538 not as completely conserved as the three tryptophan residues forming the "Trp-
539 prism" of OpuAC, changes of His^{230} in OpuAC-related proteins occur only by
540 amino acids that are capable of forming salt bridges or hydrogen bonds (20).

541 **CONCLUSIONS**

542 Site-directed mutagenesis of compatible solute binding proteins ((14, 40)
543 and this study) has demonstrated that individual amino acids within the aromatic
544 scaffold make different contributions to ligand binding. Furthermore, the strength
545 of the cation-π interaction is a key factor for the efficiency of ligand binding (14).
546 In addition to cation-π interactions, interactions between the carboxylate of the
547 substrates and the ligand binding protein permit the precise positioning of the
548 compatible solute within the binding site. As shown in this study, loss of the
549 interaction between His^{230} of OpuAC and the carboxylate of glycine betaine or
550 DMSA results in a substantial drop of affinity (Table 1). Thus, the correct

positioning of the ligand within the binding cavity requires molecular interactions involving both the positively charged head group and the negatively charged carboxylic tail of these organic solutes. Therefore, a limited set of molecular interactions is used in various compatible solute-binding proteins to precisely position the ligand within the binding site and a modulation of the interplay between these interactions generates different hierarchies in substrate affinity.

ACKNOWLEDGEMENTS

We are indebted to Matthew Groves for his excellent support during data acquisition at beamline BW-7B, EMBL Outstation Hamburg. M. H. is a recipient of a PhD fellowship from the International Max-Planck Research School (MPI Marburg). This work was supported by the Fonds der chemischen Industrie (to E. B.), the Deutsche Forschungsgemeinschaft (SFB 395 to E. B.), the Max-Planck Institut für terrestrische Mikrobiologie (Marburg) (to E.B) and grants of the Heinrich Heine University Düsseldorf (to L. S.).

References

1. **Ames, G. F.-L.** 1992. Bacterial periplasmatic permeases as a model sytem for the superfamily of traffic ATPases, including the multidrug resistance protein and the cytic fibrosis transmembrane conductance regulator. Int. Rev. Cytol. **137A:**1-35.

2. **Baliarda, A., T. Robert, M. Jebbar, C. Blanco, A. Deschamps, and C. Le Marrec.** 2003. Potential osmoprotectans for the lactic acid bacteria *Pediococcus pentosaceus* and *Tetragenococcus halophila*. Int. J. Food Microbiol. **84:**13-20.

3. **Boch, J., B. Kempf, and E. Bremer.** 1994. Osmoregulation in *Bacillus subtilis*: synthesis of the osmoprotectant glycine betaine from exogenously provided choline. J Bacteriol **176:**5364-5371.

4. **Bremer, E.** 2002. Adaptation to changing osmolarity, p. 385-391. *In* A. L. Sonenshein, J. A. Hoch, and R. Losick (ed.), *Bacillus subtilis* and its closest relatives. ASM Press, Washington, D.C.

5. **Bremer, E., and R. Krämer.** 2000. Coping with osmotic challenges: osmoregulation through accumulation and release of compatible solutes in bacteria, p. 79-97. *In* G. Storz and R. Hengge-Aronis (ed.), Bacterial stress responses. ASM, Washington, D.C.

6. **CCP4.** 1994. The CCP4 suite: programs for protein crystallography. Acta Crystallogr D **50:**760-763.

7. **Chambers, S. T., and C. M. Kunin.** 1987. Isolation of glycine betaine and proline betaine from human urine. Journal of Clinical Investigations **79:**731-737.

8. **Choquet, G., N. Jehan, C. Pissavin, C. Blanco, and M. Jebbar.** 2005. OusB, a broad-specificity ABC-type transporter from *Erwinia chrysanthemi*, mediates uptake of glycine betaine and choline with a high affinity. Appl. Environ. Microbiol. **71:**3389-3398.

9. **Cosquer, A., V. Pichereau, J. A. Pocard, J. Minet, M. Cormier, and T. Bernard.** 1999. Nanomolar levels of dimethylsulfoniopropionate, dimethylsulfonioacetate, and glycine betaine are sufficient to confer osmoprotection to *Escherichia coli*. Appl. Environ. Microbiol. **65:**3304-3311.

10. **Diab, F., T. Bernard, A. Bazire, D. Haras, C. Blanco, and M. Jebbar.** 2006. Succinate-mediated catabolite repression control on the production of glycine betaine catabolic enzymes in *Pseudomonas aeruginos* PAO1 under low and elevated salinities. Microbiology **152:**1395-1406.

11. **Dougherty, D. A.** 1996. Cation-pi interactions in chemistry and biology: a new view of benzene, Phe, Tyr, and Trp. Science **271:**163-168.

12. **Emsley, P., and K. Cowtan.** 2004. Coot: model-building tools for molecular graphics. Acta Crystallogr D **60:**2126-2132.

13. **Ferger, M. F., and V. Vigneaud.** 1950. Oxidation in vivo of the methyl groups of choline, betaine, dimethylthetin, and dimethyl-ß-propiothetin. J.

610 Biol. Chem. **185:**53-57.

611 14. **Hanekop, N., M. Hoing, L. Sohn-Bosser, M. Jebbar, L. Schmitt, and E.**
612 **Bremer.** 2007. Crystal Structure of the Ligand-Binding Protein EhuB from
613 *Sinorhizobium meliloti* Reveals Substrate Recognition of the Compatible
614 Solutes Ectoine and Hydroxyectoine. J Mol Biol **374:**1237-1250.

615 15. **Harwood, C. R., and A. R. Archibald.** 1990. Growth, maintenance and
616 general techniques, p. 1-26. *In* C. R. Harwood and S. M. Cutting (ed.),
617 Molecular biological methods for *Bacillus*. John Wiley & Sons, Inc.,
618 Chichester, UK.

619 16. **Higgins, C. F.** 1992. ABC transporters: From microorganisms to man.
620 Annu. Rev. Cell Biol. **8:**67-113.

621 17. **Horn, C., E. Bremer, and L. Schmitt.** 2005. Functional overexpression and
622 in vitro assembly of OpuA, an osmotically regulated ABC-transporter from
623 *Bacillus subtilis*. FEBS Lett. **579:**5765-5768.

624 18. **Horn, C., E. Bremer, and L. Schmitt.** 2003. Nucleotide dependent
625 monomer/dimer equilibrium of OpuAA, the nucleotide-binding protein of
626 the osmotically regulated ABC transporter OpuA from *Bacillus subtilis*. J
627 Mol Biol **334:**403-419.

628 19. **Horn, C., S. Jenewein, L. Sohn-Bosser, E. Bremer, and L. Schmitt.**
629 2005. Biochemical and structural analysis of the *Bacillus subtilis* ABC
630 transporter OpuA and its isolated subunits. J Mol Microbiol Biotechnol
631 **10:**76-91.

20. **Horn, C., L. Sohn-Bosser, J. Breed, W. Welte, L. Schmitt, and E. Bremer.** 2006. Molecular determinants for substrate specificity of the ligand-binding protein OpuAC from *Bacillus subtilis* for the compatible solutes glycine betaine and proline betaine. J Mol Biol **357:**592-606.

21. **Jebbar, M., L. Sohn-Bosser, E. Bremer, T. Bernard, and C. Blanco.** 2005. Ectoine-induced proteins in *Sinorhizobium meliloti* include an Ectoine ABC-type transporter involved in osmoprotection and ectoine catabolism. J Bacteriol **187:**1293-1304.

22. **Kappes, R. M., B. Kempf, and E. Bremer.** 1996. Three transport systems for the osmoprotectant glycine betaine operate in *Bacillus subtilis*: characterization of OpuD. J Bacteriol **178:**5071-5079.

23. **Kappes, R. M., B. Kempf, S. Kneip, J. Boch, J. Gade, J. Meier-Wagner, and E. Bremer.** 1999. Two evolutionarily closely related ABC transporters mediate the uptake of choline for synthesis of the osmoprotectant glycine betaine in *Bacillus subtilis*. Mol Microbiol **32:**203-216.

24. **Kempf, B., and E. Bremer.** 1995. OpuA, an osmotically regulated binding protein-dependent transport system for the osmoprotectant glycine betaine in *Bacillus subtilis*. J Biol Chem **270:**16701-16713.

25. **Kempf, B., and E. Bremer.** 1998. Uptake and synthesis of compatible solutes as microbial stress responses to high-osmolality environments. Arch Microbiol **170:**319-330.

26. **Kempf, B., J. Gade, and E. Bremer.** 1997. Lipoprotein from the

osmoregulated ABC transport system OpuA of *Bacillus subtilis:* purification of the glycine betaine binding protein and characterization of a functional lipidless mutant. J Bacteriol **179:**6213-6220.

27. **Kleywegt, G. J.** 1996. Use of non-crystallographic symmetry in protein structure refinement. Acta Crystallogr D **52:**842-857.

28. **Kleywegt, G. J., and T. A. Jones.** 2002. Homo crystallographicus--quo vadis? Structure **10:**465-472.

29. **Ko, R., and L. T. Smith.** 1999. Identification of an ATP-driven, osmoregulated glycine betaine transport system in *Listeria monocytogenes*. Appl Environ Microbiol **65:**4040-4048.

30. **Li, A. J., and R. Nussinov.** 1998. A set of van der Waals and coulombic radii of protein atoms for molecular and solvent-accessible surface calculation, packing evaluation, and docking. Proteins **32:**111-127.

31. **Ma, J. C., and D. A. Dougherty.** 1997. The Cation-pi Interaction. Chem Rev **97:**1303-1324.

32. **Mao, B., M. R. Pear, J. A. McCammon, and F. A. Quiocho.** 1982. Hinge-bending in L-arabinose-binding protein. The "Venus's-flytrap" model. J Biol Chem **257:**1131-1133.

33. **Miller, J. H.** 1992. A short course in bacterial genetics. A laboratory manual and handbook for *Escherichia coli* and related bacteria. Cold Spring Harbor, New York.

34. **Murshudov, G., A. A. Vagin, and E. J. Dodson.** 1997. Refinement of macromolecular structures by the maximum-likelihood method. Acta Crystallogr D **53:**240-255.

35. **Navaza, J.** 1994. AMoRe: an automated package for molecular replacement. Acta Crystallogr D **50:**157-163.

36. **Obis, D., A. Guillot, J. C. Gripon, P. Renault, A. Bolotin, and M. Y. Mistou.** 1999. Genetic and biochemical characterization of a high-affinity betaine uptake system (BusA) in *Lactococcus lactis* reveals a new functional organization within bacterial ABC transporters. J Bacteriol **181:**6238-6246.

37. **Otwinowski, Z., and W. Minor.** 1997. Processing of X-ray diffraction data collected in oscillation mode. *In* C. W. Carter and R. M. Sweet (ed.), Meth. Enzymol., vol. 276. Academic Press, London.

38. **Pichereau, V., J. A. Pocard, J. Hamelin, C. Blanco, and T. Bernard.** 1998. Differential effects of dimethylsulfoniopropionate, dimethylsulfonioacetate, and other S-methylated compounds on the growht of *Sinorhizobium meliloti* at low and high osmolarities. . Appl. Environ. Microbiol. **64:**1420-1429.

39. **Quiocho, F. A., and P. S. Ledvina.** 1996. Atomic structure and specificity of bacterial periplasmic receptors for active transport and chemotaxis: variation of common themes. Mol Microbiol **20:**17-25.

40. **Schiefner, A., J. Breed, L. Bosser, S. Kneip, J. Gade, G. Holtmann, K.**

Diederichs, W. Welte, and E. Bremer. 2004. Cation-pi interactions as determinants for binding of the compatible solutes glycine betaine and proline betaine by the periplasmic ligand-binding protein ProX from *Escherichia coli*. J Biol Chem **279:**5588-5596.

41. **Schmidt, S., K. Pfluger, S. Kogl, R. Spanheimer, and V. Muller.** 2007. The salt-induced ABC transporter Ota of the methanogenic archaeon *Methanosarcina mazei* Go1 is a glycine betaine transporter. FEMS Microbiol Lett **277:**44-49.

42. **Schmitt, L., and R. Tampé.** 2002. Structure and mechanism of ABC-transporters. Cur. Opin. Struc. Biol. **12:**754-760.

43. **van der Heide, T., and B. Poolman.** 2002. ABC transporters: one, two or four extracytoplasmic substrate-binding sites? EMBO Rep **3:**938-943.

44. **van der Heide, T., and B. Poolman.** 2000. Osmoregulated ABC-transport system of *Lactococcus lactis* senses water stress via changes in the physical state of the membrane. Proc Natl Acad Sci U S A **97:**7102-7106.

45. **Wilkinson, A. J., and K. H. G. Verschueren.** 2003. Crystal structures of periplasmic solute binding proteins in ABC transport complexes illuminate their function. *In* I. B. Holland, S. P. Cole, and K. Kuchler (ed.), ABC proteins from bacteria to man. Academic press, Amsterdam.

Table legends

TABLE 1. Using a fluorescence-based assay, the dissociation constants of glycine betaine, proline betaine and DMSA were determined for the wild type protein and each of the generated OpuAC variants. Reported K_D values are the average of at least three independent experiments with the standard deviation reported as error. >> 5 mM: no binding of ligand was detected up to the highest concentration employed in the assay (5 mM). In the case of low affinity binders such as W72F or W178Y the final substrate concentration was 2- to 3fold higher than the K_D value. Abbreviations: A: alanine, F: phenylalanine, Y: tyrosine.

TABLE 2. Crystal parameters and data collection statistics are derived from SCALEPACK (37). Refinement statistics were obtained from REFMAC5 (34) and Ramachandran analysis was performed using MolProbity. Data in parentheses correspond to the highest resolution shell (2.85- 2.80 Å).

[a] R_{sym} is defined as $R_{sym} = \sum_{hkl}\sum_{i}\left|I_i(hkl) - \langle I(hkl)\rangle\right| \Big/ \sum_{hkl}\sum_{i} I_i(hkl)$ and R_F as

[b] $R_f = \sum_{hkl}\left||F_{obs}| - |F_{calc}|\right| \Big/ \sum_{hkl}|F_{obs}|$. R_{free} is calculated as R_F but for 5% randomly chosen reflections that were omitted from all refinement steps. All amino acids located in the disallowed region of the Ramachandran plot (0.9% or 9 residues) are involved in crystal contacts.

738 TABLE 1. Dissociation constants of glycine betaine, proline betaine and

739 DMSA to the wild type OpuAC protein and its mutant derivatives.

AMINO ACID	MUTATION	GLYCINE BETAINE	PROLINE BETAINE	DMSA
Wild type		22 µM ± 4 µM	267 µM ± 6 µM	102 µM ± 11 µM
Trp^{72}	A	>> 5 mM	>> 5 mM	>> 5 mM
	F	1.4 mM ± 0.4 mM	>> 5 mM	>> 5 mM
	Y	750 µM ± 8 µM	>> 5 mM	>> 5 mM
Trp^{178}	A	>> 5 mM	>> 5 mM	>> 5 mM
	F	14 µM ± 1.4 µM	243 µM ± 28 µM	56 µM ± 17 µM
	Y	548 µM ± 263 µM	58 µM ± 27 µM	>> 5 mM
Trp^{225}	A	>> 5 mM	>> 5 mM	>> 5 mM
	F	308 µM ± 18 µM	1.93 mM ± 0.03 mM	>> 5 mM
	Y	67 µM ± 22 µM	1.25 mM ± 0.28 mM	425 µM ± 30 µM
His^{230}	A	392 µM ± 92 µM	491 µM ± 195 µM	259 µM ± 55 µM
$Trp^{72/178}$	F	>> 5 mM	>> 5 mM	>> 5 mM
	Y	>> 5 mM	>> 5 mM	>> 5 mM
$Trp^{72/225}$	F	>> 5 mM	>> 5 mM	>> 5 mM
	Y	>> 5 mM	>> 5 mM	>> 5 mM
$Trp^{72/178/225}$	F	>> 5 mM	>> 5 mM	>> 5 mM
	Y	>> 5 mM	>> 5 mM	>> 5 mM

740 TABLE 2. Data collection and refinement statistics for the OpuAC/DMSA

741 complex.

Crystal parameters at 100 K	
Space group	$P2_1$
Unit Cell parameters	56.51, 150.61, 58.96
a, b, c (Å)	90.0, 104.54, 90.0
α, β, γ (deg.)	
B. Data collection and processing	
Wavelength (Å)	0.98
Resolution (Å)	20-2.8 (2.85-2.8)
Mean redundancy	2.4
Unique reflections	24,818
Mosaicity (°)	0.4
Completeness (%)	93.0 (96.5)
I/σ	6.8 (3.0)
R_{merge}[a]	16.4 (28.8)
C. Refinement	
R_F[b] (%)	28.5
R_{free}[c] (%)	36.4
Overall B-factor from Wilson scaling (Å^2)	27.4
rmsd from ideal	
Bond lengths (Å)	0.07
Bond angles (deg.)	1.12
Average B-factors (Å^2)	27.85
Ramachandran plot	
Most favored (%)	89.2
Allowed (%)	9.9
Generously allowed (%)	
Disallowed (%)	0.9
D. Model content	
Monomers/ASU	4
Protein residues	20-272
Ligand	Four DMSA

742

Figure legends

FIG. 1. Chemical structures of the OpuAC substrates used in this study.

FIG. 2. Osmoprotective effects of the compatible solutes glycine betaine and DMSA for *B. subtilis*. A. The OpuA$^+$ (OpuB$^-$ OpuC$^-$ OpuD$^-$) strain RMKB34 was grown in SMM with 1.2 M NaCl (–■–), 1.2 M NaCl with 1 mM glycine betaine (–●–) and 1.2 M NaCl with 1 mM DMSA (–▲–). B. The OpuA$^-$ (OpuB$^-$ OpuC$^-$ OpuD$^-$) strain RMKB24 was grown in SMM with 1.2 M NaCl (–■–), 1.2 M NaCl with 1 mM glycine betaine (–▲–) and 1.2 M NaCl with 1 mM DMSA (–●–). Cultures (20 ml) were inoculated to an OD_{578} of 0.1 from overnight cultures pre-grown in SMM with 0.4 M NaCl and were propagated in 100-ml Erlenmeyer flasks in a shaking water bath (220 rpm) at 37°C. Cell growth was monitored over time by measuring the OD_{578}.

FIG. 3. Ligand binding of OpuAC with DMSA (A, B). (A) Emission spectra of the protein in the absence (red line) or presence (black, dashed line) of 1 mM substrate. (B) Equilibrium binding titration experiments with DMSA.

FIG. 4. View of the ligand-binding pocket of the OpuAC/DMSA complex. Interactions between the OpuAC protein and its ligand DMSA are highlighted by dashed lines. Highlighted are the three tryptophans (Trp^{72}, Trp^{178}, Trp^{225}) and the histidine residue (His^{230}), which constitute the binding pocket. Amino acids given

766 in single letter code in brackets indicate the mutations performed in this study.

767

768 FIG. 5. View of the superpositioning of the ligand-binding sites of the
769 OpuAC/glycine betaine, OpuAC/proline betaine and OpuAC/DMSA complexes.
770 Residues involved in glycine betaine coordination are shown in green, residues
771 involved in proline betaine binding are shown in orange and the residues involved
772 in DMSA binding are shown in purple. For simplicity, the backbone contacts of
773 the ligands with Gly^{26} and Ile^{27} have been omitted from the representation.

774

775 FIG. 6. Domain organization of glycine betaine binding proteins related to OpuAC
776 from *B. subtilis*. Data base searches using the BLAST program showed that there
777 are four classes of ligand binding proteins that are related to OpuAC from *B.*
778 *subtilis*. The OpuAC-protein from *B. subtilis* is shown with the residues involved
779 in binding of the trimethylammonium-headgroup of glycine betaine (W72, W178,
780 W225) and the carboxylate of glycine betaine (G26, I27, H230). Group 1 contains
781 those proteins that align directly with the OpuAC-protein. An example is the
782 glycine betaine binding protein GbuC from *Listeria monocytogenes* (29). Group 2
783 is composed of proteins that align with the OpuAC-protein when the N- and C-
784 terminal domains are inverted. An example is the glycine betaine binding protein
785 OtaC from the archaeon *Methanosarcina mazei* (41). Binding protein domains
786 that are fused to the transmembrane domain of the ABC-transport system and
787 contain the domain inversion form group 3. An example is the glycine betaine
788 binding/transmembrane protein OpuBC (also referred to as BusAB) from

Lactococcus lactis (36, 44). Finally, group 4 of the OpuAC related proteins contain those examples where the transmembrane domain is fused to a duplicated binding protein domain both of which contain the domain inversion. This type of fusion protein was first noticed by van der Heide and Poolman (43). An example of this group of OpuAC related-proteins is present in *Streptomyces coelicolor* (NP_625895). But in contrast to the other mentioned glycine betaine binding proteins, the substrate specificity of this fused binding protein has not been experimentally assessed. For the various alignments, the N-terminal and C-terminal domains of OpuAC were split between the amino acids 168/169 as initially described by Horn *et al*. (20).

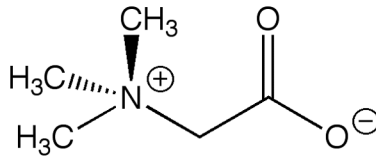

Glycine betaine

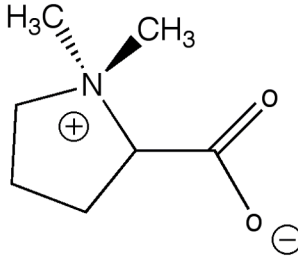

Proline betaine

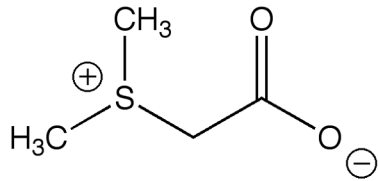

DMSA

A

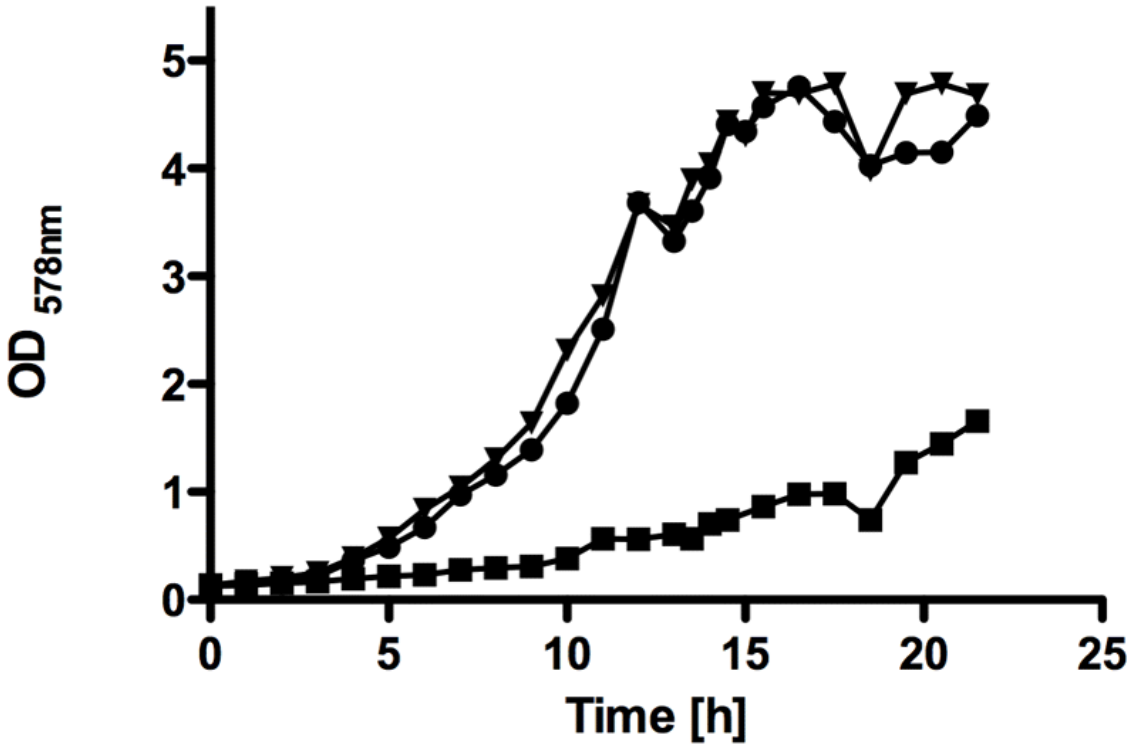
OD 578nm
0
1
2
3
4
5
0
5
10
15
20
25
Time [h]

B

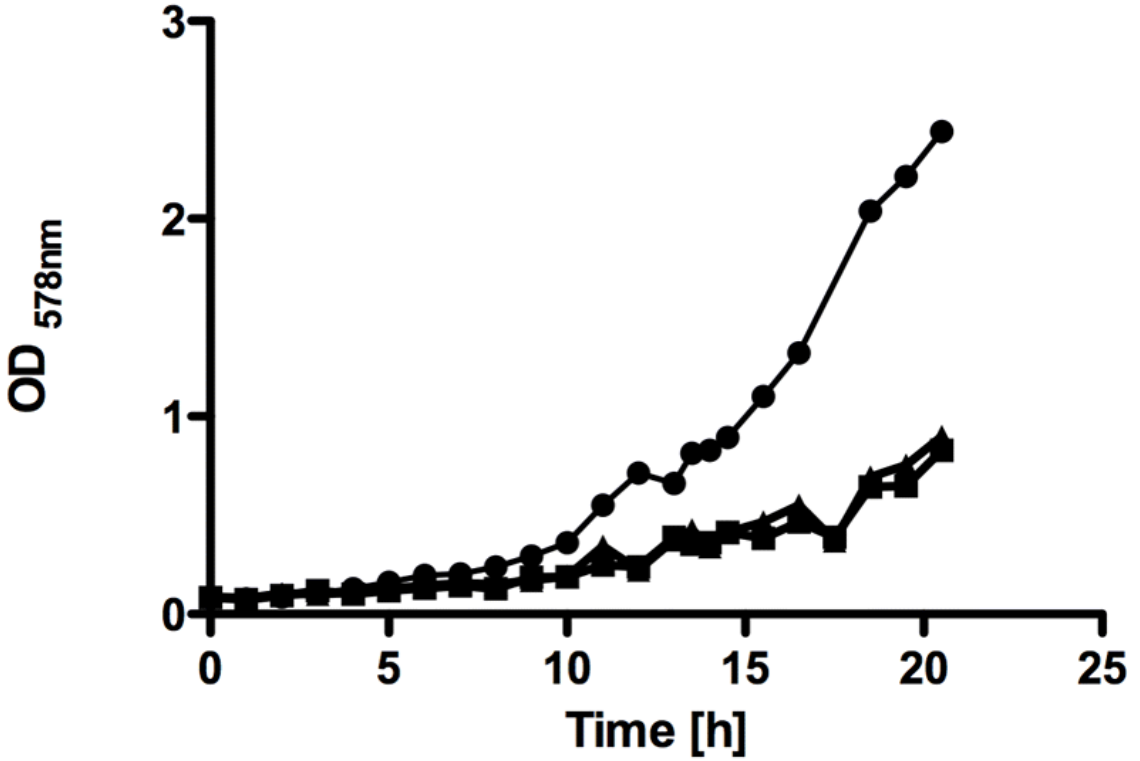
OD 578nm
0
1
2
3
0
5
10
15
20
25
Time [h]

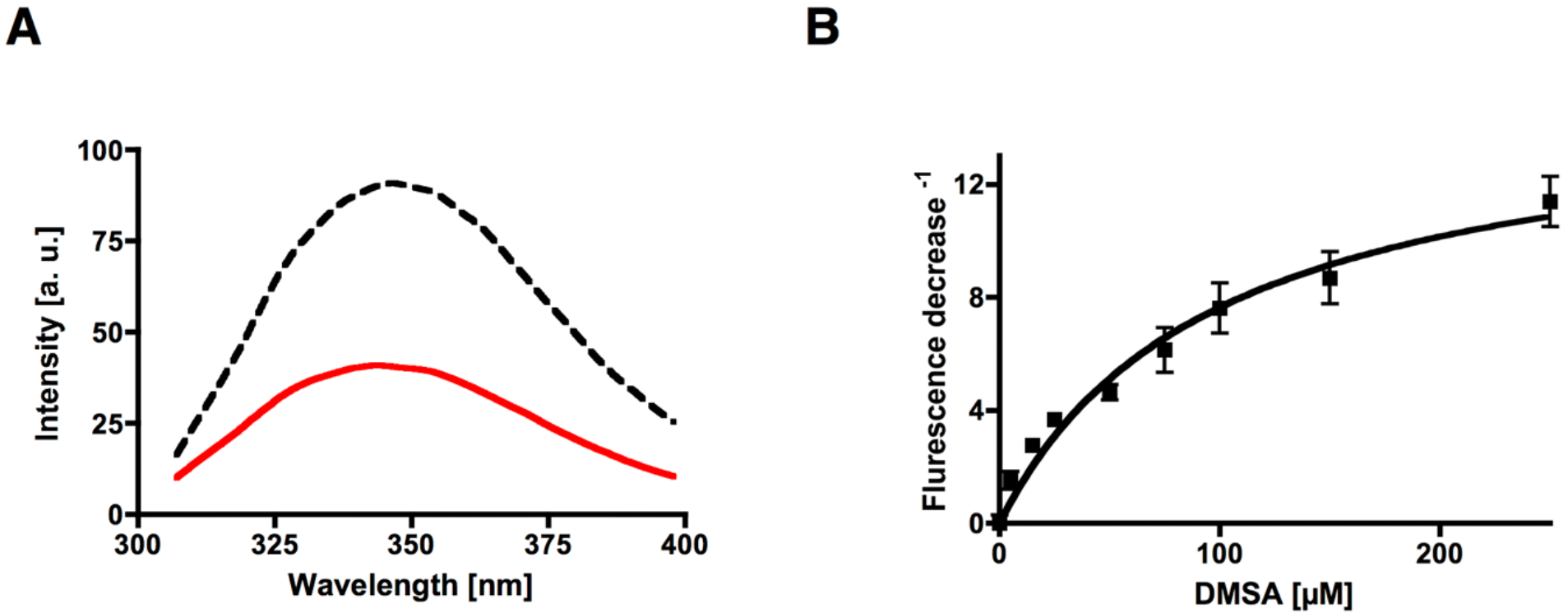
A
100
75
50
25
0
Intensity [a. u.]
300
325
350
375
400
Wavelength [nm]
B
12
8
4
0
Flurescence decrease -1
0
100
200
DMSA [μM]

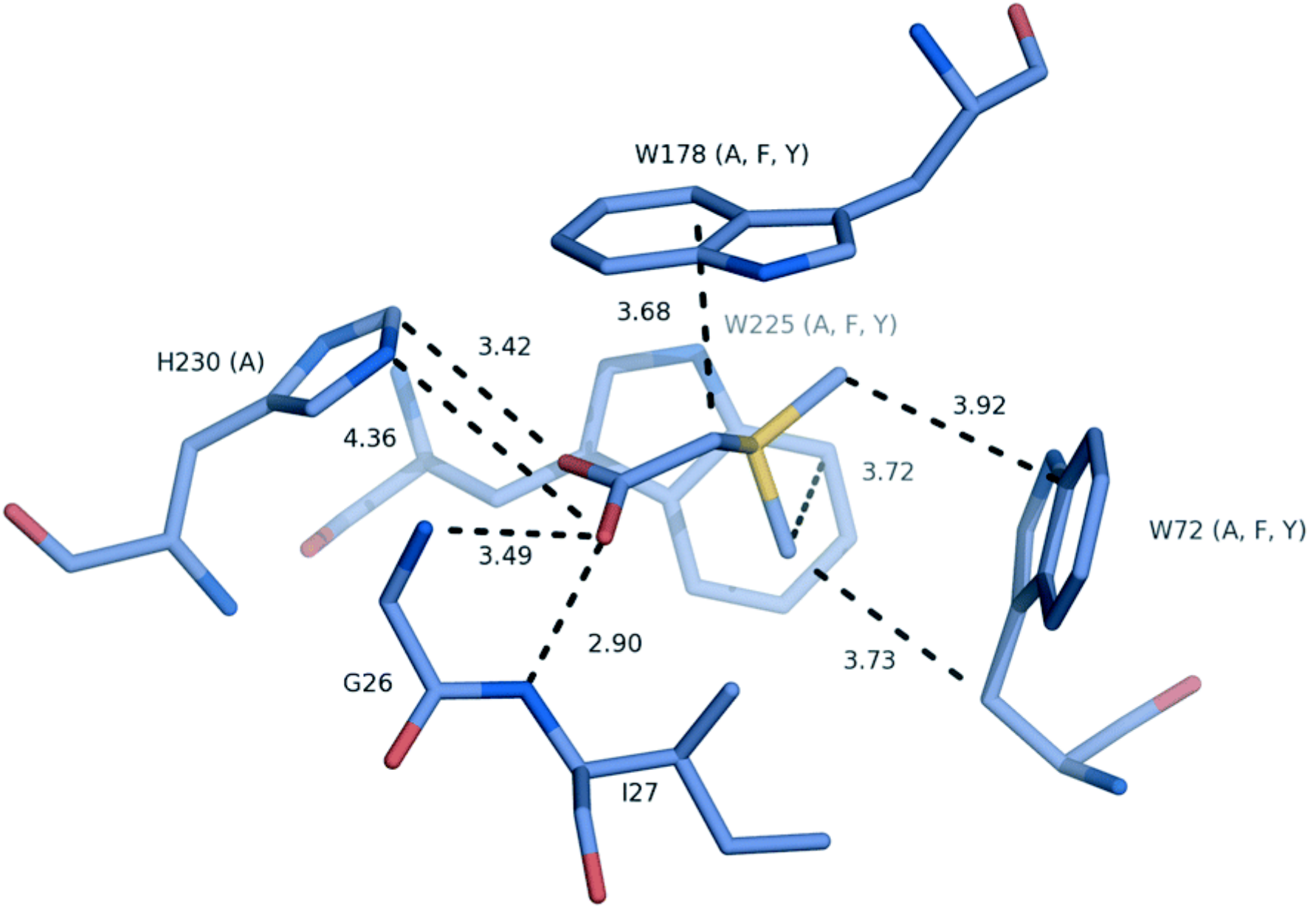
W178 (A, F, Y)
3.68
W225 (A, F, Y)
H230 (A)
3.42
4.36
3.92
3.72
W72 (A, F, Y)
3.49
2.90
3.73
G26
I27

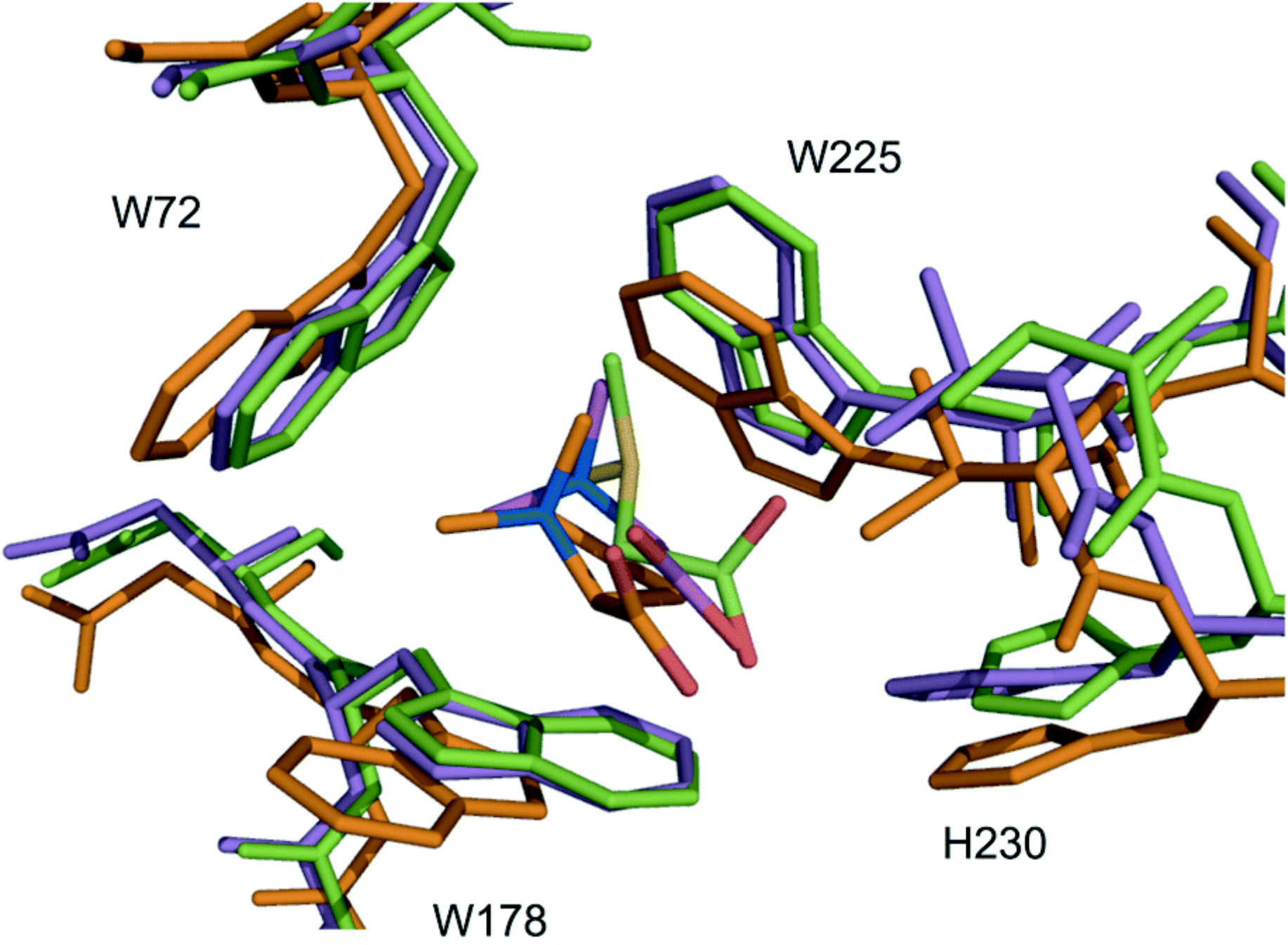
W72
W225
H230
W178

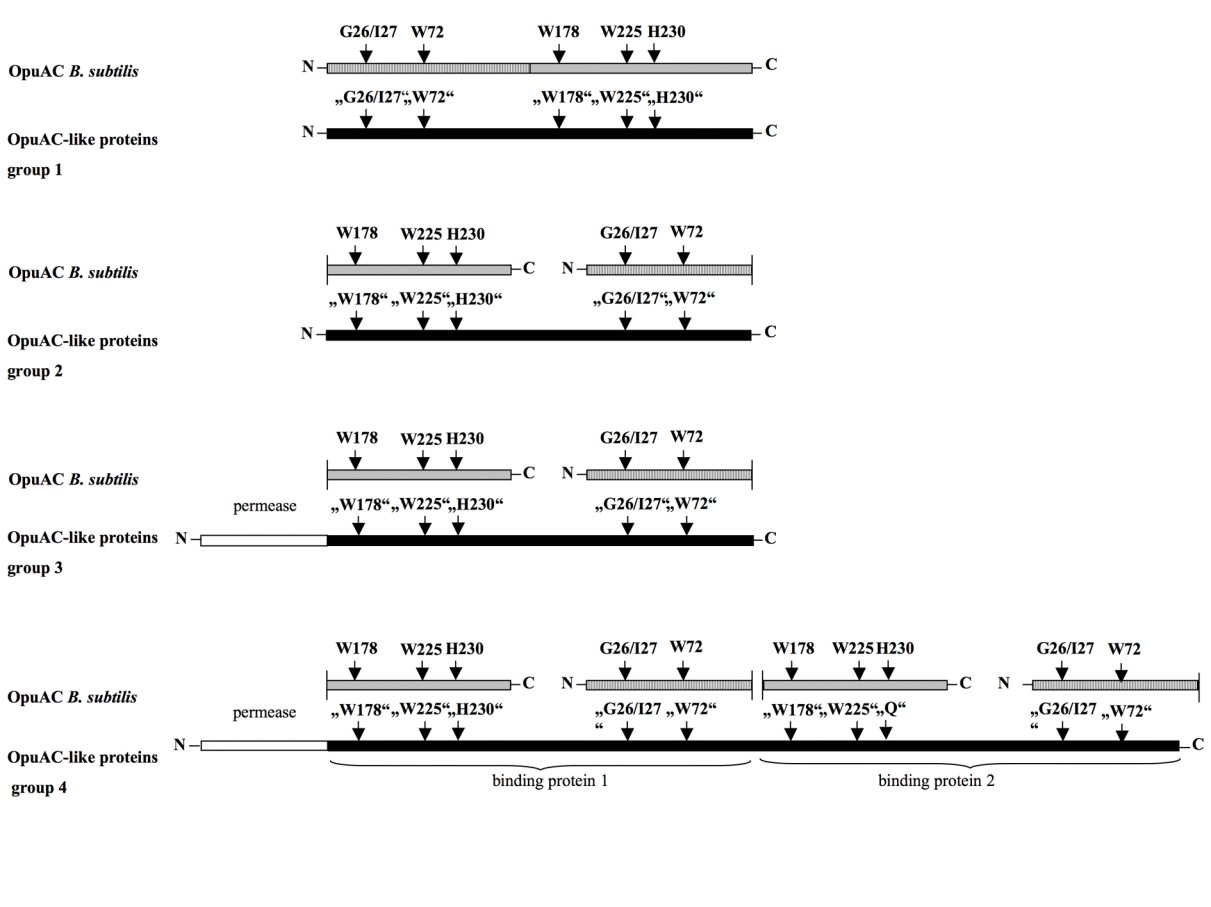
OpuAC B. subtilis
G26/I27 W72
W178 W225 H230
N
C
OpuAC-like proteins
group 1
„G26/I27“„W72“
„W178“„W225“„H230“
OpuAC B. subtilis
W178 W225 H230
G26/I27 W72
OpuAC-like proteins
group 2
„W178“ „W225“„H230“
„G26/I27“„W72“
OpuAC B. subtilis
permease
OpuAC-like proteins
group 3
OpuAC B. subtilis
permease
„W178“„W225“„H230“
„G26/I27 „W72“
„W178“„W225“„Q“
OpuAC-like proteins
group 4
binding protein 1
binding protein 2